Available online at www.sciencedirect.com
ScienceDirect
Biochimica et Biophysica Acta 1778 (2008) 824–834
Biochimica et Biophysica Acta
BBA
www.elsevier.com/locate/bbamem

Comparison of rat epidermal keratinocyte organotypic culture (ROC) with intact human skin: Lipid composition and thermal phase behavior of the stratum corneum

Sari Pappinen [a], Martin Hermansson [b], Judith Kuntsche [a,c], Pentti Somerharju [b], Philip Wertz [d], Arto Urtti [a,e], Marjukka Suhonen [a,*]

[a] Department of Pharmaceutics, University of Kuopio, P.O. Box 1627, 70211 Kuopio, Finland
[b] Institute of Biomedicine, Department of Biochemistry, University of Helsinki, P.O. Box 63, 00014 Helsinki, Finland
[c] Department of Pharmaceutical Technology, Martin-Luther-University Halle, 06120 Halle/Saale, Germany
[d] Dows Institute, University of Iowa, Iowa City IA 52242, USA
[e] Drug Discovery and Development Technology Center, University of Helsinki, P.O. Box 56, 00014 University of Helsinki, Finland

Received 6 February 2007; received in revised form 19 December 2007; accepted 24 December 2007
Available online 4 January 2008

Abstract

The present report is a part of our continuing efforts to explore the utility of the rat epidermal keratinocyte organotypic culture (ROC) as an alternative model to human skin in transdermal drug delivery and skin irritation studies of new chemical entities and formulations. The aim of the present study was to compare the stratum corneum lipid content of ROC with the corresponding material from human skin. The lipid composition was determined by thin-layer chromatography (TLC) and mass-spectrometry, and the thermal phase transitions of stratum corneum were studied by differential scanning calorimetry (DSC). All major lipid classes of the stratum corneum were present in ROC in a similar ratio as found in human stratum corneum. Compared to human skin, the level of non-hydroxyacid-sphingosine ceramide (NS) was increased in ROC, while α-hydroxyacid-phytosphingosine ceramide (AP) and non-hydroxyacid-phytosphingosine ceramides (NP) were absent. Also some alterations in fatty acid profiles of ROC ceramides were noted, e.g., esterified ω-hydroxyacid-sphingosine contained increased levels of oleic acid instead of linoleic acid. The fraction of lipids covalently bound to corneocyte proteins was distinctly lower in ROC compared to human skin, in agreement with the results from DSC. ROC underwent a lipid lamellar order to disorder transition (T_2) at a slightly lower temperature (68 °C) than human skin (74 °C). These differences in stratum corneum lipid composition and the thermal phase transitions may explain the minor differences previously observed in drug permeation between ROC and human skin.

Keywords: ROC; Reconstructed epidermis; Stratum corneum; Lipid composition; DSC; TLC

1. Introduction

The uppermost layer of the skin, i.e. stratum corneum, is known to provide a barrier against water loss and to prevent the intrusion of microorganisms and chemicals. Epidermal keratinocyte proliferation, differentiation and cell death occur sequentially, and the stratum corneum represents the final stage of the differentiation process. Dead corneocytes are filled with keratin filaments and enclosed in highly organized lipid lamellae [1].

During differentiation, the epidermal lipid content and composition change dramatically in the interface of stratum granulosum

Abbreviations: AS, α-hydroxyacid-sphingosines; AP, α-hydroxyacid-phytosphingosines; AH, α-hydroxyacid-6-OH-sphingosines; DSC, differential scanning calorimetry; EOS, ω-*O*-acyl-hydroxyacid-sphingosine; EOP, ω-*O*-acyl-hydroxyacid-phytosphingosine; EOH, ω-*O*-acyl-hydroxyacid-6-OH-sphingosine; FFA, free fatty acid; NS, non-hydroxyacid-sphingosines; NP, non-hydroxyacid-phytosphingosines; NH, non-hydroxyacid-6-OH-sphingosines; REK, rat epidermal keratinocyte; ROC, REK organotypic culture; TLC, thin-layer chromatography

* Corresponding author. Tel.: +358 17 163454; fax: +358 17 162252.
E-mail address: Marjukka.Suhonen@uku.fi (M. Suhonen).

0005-2736/$ - see front matter © 2008 Elsevier B.V. All rights reserved.
doi:10.1016/j.bbamem.2007.12.019

and stratum corneum. Lipid precursors (mainly phospholipids, cholesterol and glucosylceramides) are enclosed into vesicles, lamellar bodies, in the granular cells [2,3]. After the extrusion of lamellar bodies at the interface of stratum granulosum and stratum corneum, polar lipids are enzymatically converted into more apolar products; phosphoglycerides to free fatty acids, and sphingomyelin and glucosylceramides to ceramides [4]. These lipids and cholesterol then form the lipid lamellae with their characteristic orthorhombic lateral organization and repeating pattern of 6 nm (short periodicity phase, SPP) and 13 nm (long periodicity phase, LPP) [5,6]. The stratum corneum contains an approximately equimolar ratio of cholesterol, ceramides and free fatty acids, which is important for the orthorhombic packing and formation of LPP [7]. The presence of ω-hydroxyceramides, especially esterified ω-hydroxysphingosine (EOS), is critical for the proper molecular organization of LPP structures, although the presence of all nine ceramide subclasses further supports LPP formation [8–10].

The protein rich cornified envelope finally replaces the plasma membrane of differentiated cells, and approximately two-thirds of the total ω-hydroxyceramides are covalently bound to the outer surface of envelope proteins where they form lipid–protein complexes [11–13]. These structures contain one layer of lipids bound via ester bonds to glutamic acid residues of cornified envelope protein, mainly involucrine [14]. Covalently bound ceramides are believed to serve as a template for the formation of lipid lamellae in the extracellular space. Although an elevated transepidermal water loss has been attributed to a decline in the number of covalently bound ceramides [15], the relationship between bound lipid and the barrier function of the stratum corneum is not well established.

There are several reasons why reconstructed skin models are predicted to replace the native skin in in vitro experiments; there are fewer ethical concerns, they are easy to prepare and provide more reproducible results. However, such models need to be morphologically and physiologically equivalent to human skin. To produce these models, keratinocytes can be seeded onto synthetic matrices, collagenated matrices, fibroblast containing collagen matrices or cultured on de-epidermised dermis, and are grown in an airlifted state [16–26]. Often the general ultrastructure of the model epidermis is similar to that of native skin. In the most advanced skin models, the overall lipid composition of the epidermis approaches that of native skin, but the organization of the lipid lamellae may be altered [27,28]. Also the differentiation process in many models is disturbed, as indicated by retarded lamellar body extrusion, the absence of LPP and covalently bound ceramides, the presence of intercellular lipid droplets and crystalline cholesterol as well as over- or under-expression of key proteins and enzymes [28]. This might lead to differences in the molecular composition of the individual lipid classes, which can disturb normal lipid packaging. One such difference is the substitution of linoleate for oleate in EOS [19,29]. Although the lipid composition and arrangement in skin models can be improved by modifying the culture conditions [30,31], many reports have revealed that these skin models are still significantly more permeable than human skin [18,32–35].

The rat epidermal keratinocyte organotypic culture (ROC) is a three-dimensional skin model that exhibits a normal stratum corneum ultrastructure and functional properties [26,36]. It has been shown to (i) form a drug permeability barrier very similar to that of human skin [37], (ii) correctly predict the skin irritation potential of topically applied chemicals [38], (iii) respond to dermal penetration enhancers in the same way as human skin [39], (iv) be useful as a tool for dermal gene delivery studies [40] and (v) mimic skin in iontophoretic studies (Raiman, J. et al., University of Helsinki, Division of Pharmaceutical Technology, unpublished data). The main advantage of ROC in pharmaceutical and chemical testing is its well developed permeability barrier which is often lacking in several of the cultured skin models. The lipid matrix of stratum corneum is considered to constitute the major barrier to percutaneous penetration. ROC has previously been demonstrated to contain lamellar bodies, which are completely extruded into the stratum granulosum/stratum corneum interface [26,36]. Most of the intercellular lipids form a typical repeating pattern of Landmann units [2], although there may be some abnormal lipid droplets, an anomaly not untypical for reconstructed skin models. ROC also contains the cornified envelopes and its components, such as keratin filaments, involucrine and filaggrin.

We are continuing to explore the utility of the rat epidermal keratinocyte organotypic culture (ROC) as an alternative model to human skin in transdermal drug delivery and skin irritation studies. ROC is still slightly leakier than human skin [37] and in this study we have evaluated whether this could be explained by the deviations in the lipid profiles of the stratum corneum of these two models. Therefore we compared the lipid composition of ROC and human stratum corneum in detail using thin-layer chromatography (TLC) and mass-spectrometry. In addition, the thermal behavior of ROC and human stratum corneum was investigated by differential scanning calorimetry (DSC). The results show that all of the major lipid classes typical for native skin were present in ROC in a comparable ratio as found in human stratum corneum. However, the differences in the DSC profiles indicate that the stratum corneum of human skin and ROC do differ in their structural characteristics.

2. Materials and methods

2.1. Materials

Minimal Essential Medium (MEM; without L-glutamine), Dulbecco's MEM (DMEM; with 4500 mg/l glucose), Earle's Balanced Salt Solution (EBSS, 10x) and 7.5% sodium bicarbonate solution were obtained from Gibco BRL (Life Technologies Ltd., Paisley, Scotland). PBS tablets for preparation of pH 7.4 buffer solution, penicillin–streptomycin sulfate solution, L-glutamine solution, trypsin–EDTA solution, L-ascorbic acid, trypsin type III from bovine pancreas, trypsin inhibitor type II from soybean, cholesterol, cholesterol sulfate, copper sulfate and sodium bromide were purchased from Sigma (St. Louis, MO, USA). Fetal bovine serum (FBS) was from HyClone (Logan, UT, USA). Transwell tissue culture inserts (24 mm diameter, 3.0 μm pore size) were obtained from Costar (Cambridge, MA, USA). Ceramide NS and glucosylceramide were obtained from Avanti Polar Lipids (Alabaster, Alabama, USA), and C24:0 fatty acid, acetic acid and ortho-phosphoric acid from Fluka (Buchs, Germany). *n*-Hexane and chloroform were from Rathburn Chemicals (Walkerburn, Scotland), methanol from LabScan (Dublin, Ireland) and diethylether from Baker (Deventer, Holland). Sodium hydroxide was from OY FF-Chemicals AS (Yli-Ii, Finland) and NaBr from Sigma-Aldrich (Seelze, Germany).

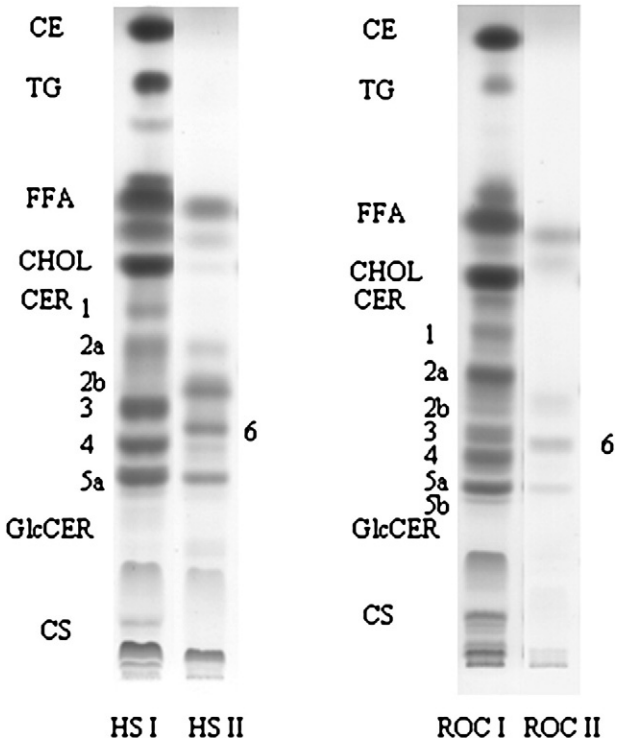

Fig. 1. TLC analysis of stratum corneum lipid composition: A representative sample for free lipids (200 μg) (I) and covalently bound ω-hydroxyceramides (II, line 6) (in similar volume to free lipids) extracts of ROC and human stratum corneum (HS) is shown. CER: ceramide; CHOL: cholesterol; CS: cholesterol sulfate; CE: cholesterol esters, FFA: free fatty acids, GlcCER: glucosylceramides, TG: triglycerides.

2.2. REK organotypic culture (ROC)

Rat epidermal keratinocyte (REK) cell line from newborn rats, which was originally isolated as previously reported [41], was used. Stock cultures were grown in MEM supplemented with 10% FBS, 4 mM L-glutamine, 50 U/ml penicillin and 50 μg/ml streptomycin sulfate at 37 °C and in 5% CO_2, according to the protocol described earlier [26,36]. For the organotypic cultures (ROC), REKs were seeded onto collagen coated Transwell culture inserts (400,000 cells/insert) using DMEM supplemented with 10% FBS, 4 mM L-glutamine, 50 U/ml penicillin, 50 μg/ml streptomycin sulfate and 40 μg/ml L-ascorbic acid at 37 °C and in 5% CO_2 as described earlier [26,36]. The cultures were grown airlifted for three weeks prior to use. The barrier integrity was monitored periodically by examining the permeation of a lipophilic compound, corticosterone, and a hydrophilic compound, mannitol, to ensure the uniformity of culture batches [37].

2.3. Isolation of stratum corneum from human skin and ROC culture

Excised human abdomen skin samples were obtained from the Kuopio University Hospital (Kuopio, Finland), within four days post-mortem. The contact of subcutaneous tissue with the stratum corneum was prevented in each step of sample preparation to avoid contamination with dermal lipids. The fat tissue was removed and the skin samples were rinsed with ice-cold hexane for 30 s to remove unwanted surface lipids [42]. The dermal side of the skin tissue was placed into contact with a 0.1% trypsin solution in PBS at 37 °C for 2–3 days and the trypsin solution was replaced by fresh solution every 24 h until the stratum corneum could be peeled off. The treatment with ice-cold hexane for 30 s was repeated and the stratum corneum was rinsed with purified water. To achieve the optimal removal of all epidermal cells, the stratum corneum sheets were treated once more with 0.1% trypsin in PBS for 2 h at 37 °C. Then the stratum corneum was peeled off and placed into a 0.1% trypsin inhibitor solution in purified water and finally rinsed with purified water. Separated stratum corneum sheets were briefly air dried and placed in a desiccator over a silica gel, under nitrogen and light protection for later use.

ROC epidermal membrane was peeled off from the culture insert and collagen support, rinsed for 30 s with ice-cold hexane in the same way as human stratum corneum and placed in 0.1% trypsin solution in PBS for 2 h at 37 °C. Thereafter, the stratum corneum was peeled off, treated with 0.1% trypsin inhibitor solution, rinsed with purified water and stored in the same way as human skin after drying at room temperature.

2.4. Extraction of lipids

About 40 mg of the dry stratum corneum was cut into small pieces and placed in a silanized Pyrex tubes (Barloworld Scientific, Staffordshire, UK). Free lipids were extracted using first three consequent extractions with chloroform/methanol in different ratios (2:1, 1:1, 1:2 v/v) as described previously [43], and finally with a single two-hour extraction with methanol. Thereafter, the remaining material was subjected to a mild alkaline hydrolysis to extract the lipids covalently bound to proteins [12]. The extract of covalently bound lipids and the combined extracts of free lipids were evaporated under nitrogen flow at room temperature, dissolved in 5 ml of chloroform/methanol (2:1 v/v) and washed with 1 ml of 0.88% KCl in water (w/v) [44]. After evaporation of the solvents under nitrogen flow, the lipids were dissolved in chloroform/methanol (2:1 v/v) at a concentration of 10 mg/ml and stored at −20 °C.

2.5. TLC analysis of lipid classes

The lipids were analyzed by a thin-layer chromatography using 20×20 cm glass plates coated with a 0.25 mm thick silica gel layer (Merck, Darmstadt, Germany). Samples of 5, 10, 15 and 20 μl of the free lipid extract and 20 μl of covalently bound lipid extract were applied to the plate. The lipids were separated by one-dimensional TLC using the following solvent systems sequentially: chloroform/methanol/water 40:10:1 (v/v/v) to 10 cm; chloroform/methanol/acetic acid 190:9:1 (v/v/v) to 16 cm; hexane/diethylether/acetic acid 70:30:1 (v/v/v) to 20 cm [45]. Before developing the plates with a new mobile phase, the plates were carefully dried under a gentle air stream. Lipid classes were identified by comparing the lipid spots of the stratum corneum samples with cholesterol, free fatty acid (C24:0), ceramide NS (C24:0), glucosylceramide and cholesterol sulfate standards. After development and drying, the plates were dipped into $CuSO_4$*7 H_2O (7.5% w/v)/phosphoric acid (8% v/v) solution and heated at 180 °C for 8 min. The plates were then laser-scanned and the integrated density of standard and sample lipid bands was quantified by Dot plot analysis of the ImageJ software (Wayne Rasband, National Institute of Health, USA). Results were calculated from standard curves.

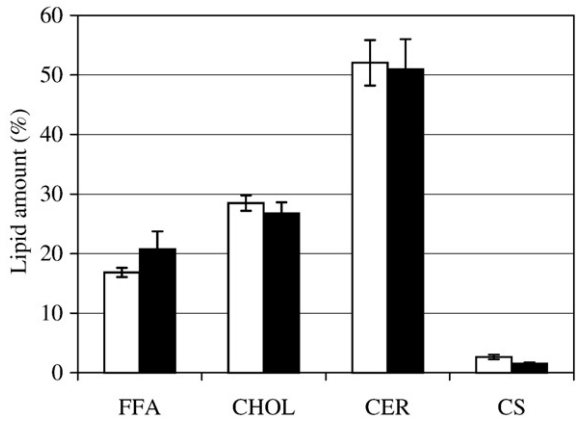

Fig. 2. Lipid composition (mean wt. %±S.D.) of stratum corneum free lipid extracts of ROC (white bars) and human skin (black bars) as determined by TLC analysis. Lipid amount: Percent of total lipid in the respective lipid class. FFA: free fatty acids, CER: ceramides; CHOL: cholesterol; CS: cholesterol sulfate (n=4–5).

Table 1
Composition of ceramide spots separated from TLC plate and analyzed by mass-spectrometry

Ceramide spot	Human stratum corneum	ROC
1	EOS	EOS
2a	NS	NS_{C22-31}
2b	EOP	NS_{C16-20}
3	NP,EOH	EOH,NH_{C28-30}
4	AS,NH	AS,NH
5a	AP,AH	AH
5b	–	AH_{C16-24}
6	OS,OH,OP	OS,OH,OP

EO = esterified ω-hydroxyacid, N = non-hydroxyacid, A = α-hydroxyacid, S = sphingosine, P = phytosphingosine, H = 6-hydroxysphingosine.

2.6. Mass-spectrometry analysis

Free and covalently bound ceramide classes separated by TLC were scraped from the plate and extracted for 5 min with ultrasonication in 3 ml of chloroform/methanol (1:1 v/v) in silanized Pyrex tubes. The extracts were first washed with 0.75 ml of purified water and then with 1 ml of chloroform/methanol/water 2:2:1 (v/v/v) upper phase [44]. The organic solvents were evaporated and the residues were dissolved in chloroform/methanol (1:2 v/v) prior to analysis. Identification of the classes and molecular species was carried out by LC-ESI-MS/MS. Chromatographic separation was carried out in the gradient mode using a Famos autosampler and Ultimate nano-HPLC apparatus (LC Packings, Amsterdam, Netherlands) equipped with a 2.1×50 mm Discovery C_{18} column (Supelco, Bellefonte, PA) packed with 5 μm particles. The solvents used were A = methanol/water/formic acid (74:25:1, v/v/v), B = methanol/formic acid (99:1 v/v) and C = chloroform/methanol/formic acid (33:66:1 v/v/v), each containing 5 mM ammonium formate. The gradient started from 100% A and was changed linearly to 100% B at 20 min, and after 10 min changed linearly to 100% C within 5 min. After 5 min, the solvent was changed linearly to 100% B in 5 min and then to 100% A in 5 min. The column was equilibrated for 10 min with 100% A prior to the next injection. The flow rate was 0.5 ml/min.

The column eluent was introduced into the electrospray source of a Quattro Micro triple-quadrupole mass-spectrometer (Micromass, Manchester, UK) operated in the positive ion mode. Nitrogen was used as the nebulizer (500 l/h at 130 °C) and cone gas (50 l/h). The source temperature was 90 °C and the potentials of the cone, extractor and RF lens were 40, 2 and 0.3 V, respectively. The precursor ion spectra were scanned from 500 to 1200 m/z at a frequency of one scan per two seconds. The ceramides were identified according to their molecular weight, characteristic fragmentation pattern [46] and elution time. After identification, the molecular species of each ceramide subclass were analyzed semi-quantitatively using direct infusion of the crude lipid extract and scanning for the precursors of the different sphingoid bases [46]. The spectra were smoothed, transferred to Microsoft Excel and the relevant peaks were quantified using the LIMSA-software recently designed for this purpose [47].

Analysis of the phospholipid classes and molecular species was carried out essentially as described previously [48]. Briefly, the different phospholipid classes were selectively detected by using head group-specific precursor ion or neutral loss scanning modes and quantified using internal standards. Phosphatidylcholines and sphingomyelins were detected by scanning for the precursors of 184 and phosphatidylethanolamines by scanning for constant neutral loss 141 in the positive ion mode. The collision energy was set to 20–55 eV and argon was used as the collision gas. The spectra were then analyzed as described above.

2.7. Differential scanning calorimetry

Dry stratum corneum sheets were hydrated over a 27% NaBr solution for 48 h to ensure 20% hydration [49]. Phase transition temperatures of the stratum corneum are known to be stable in a water content of 20% or greater [50]. The sheets were cut into small pieces and 3–4 mg were hermetically sealed in 10 μl aluminium pans and analyzed using a DSC 823^e instrument (Mettler Toledo, Schwerzenbach, Switzerland). An empty pan was used as reference. The calorimeter was calibrated using zinc, lead, indium and milli-Q water under nitrogen plugging gas flow of 50 ml/min. The samples were heated from 10 to 110 °C, cooled to 0 °C and heated up again with a scan rate of 10 °C/min. Isothermic steps with a duration of 2 min were inserted between all temperature scans. The DSC curves are normalized to the sample mass (hydrated stratum corneum) and the transition temperatures are referred to the peak maxima determined in the heating runs.

3. Results

3.1. Stratum corneum lipid composition

Stratum corneum of human skin and ROC contained 15.1±0.4% (151 μg/mg) and 12.9±1.2% (129 μg/mg) of lipids of the dry

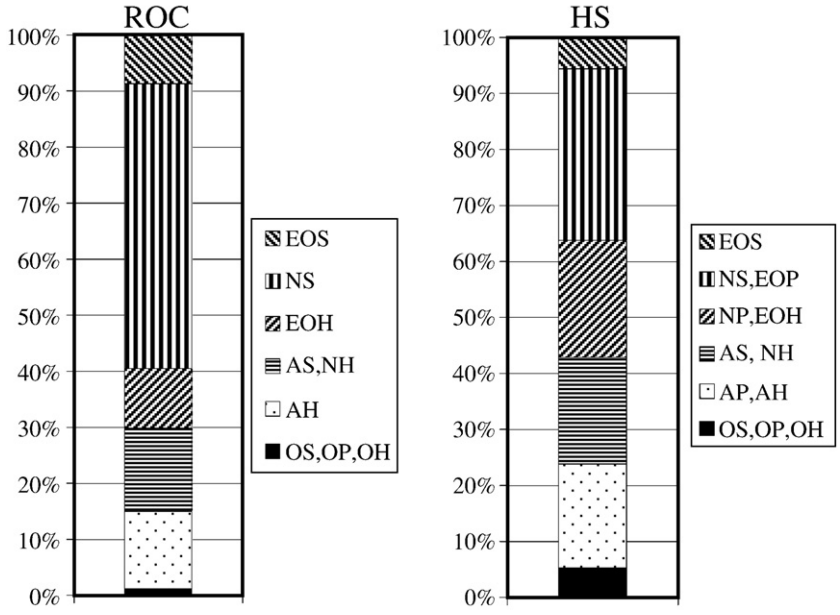

Fig. 3. Relative proportions (wt. %) of different free and covalently bound (OS,OP,OH) ceramide subclasses in stratum corneum of ROC and human skin (HS) as determined by TLC analysis (n=4–5).

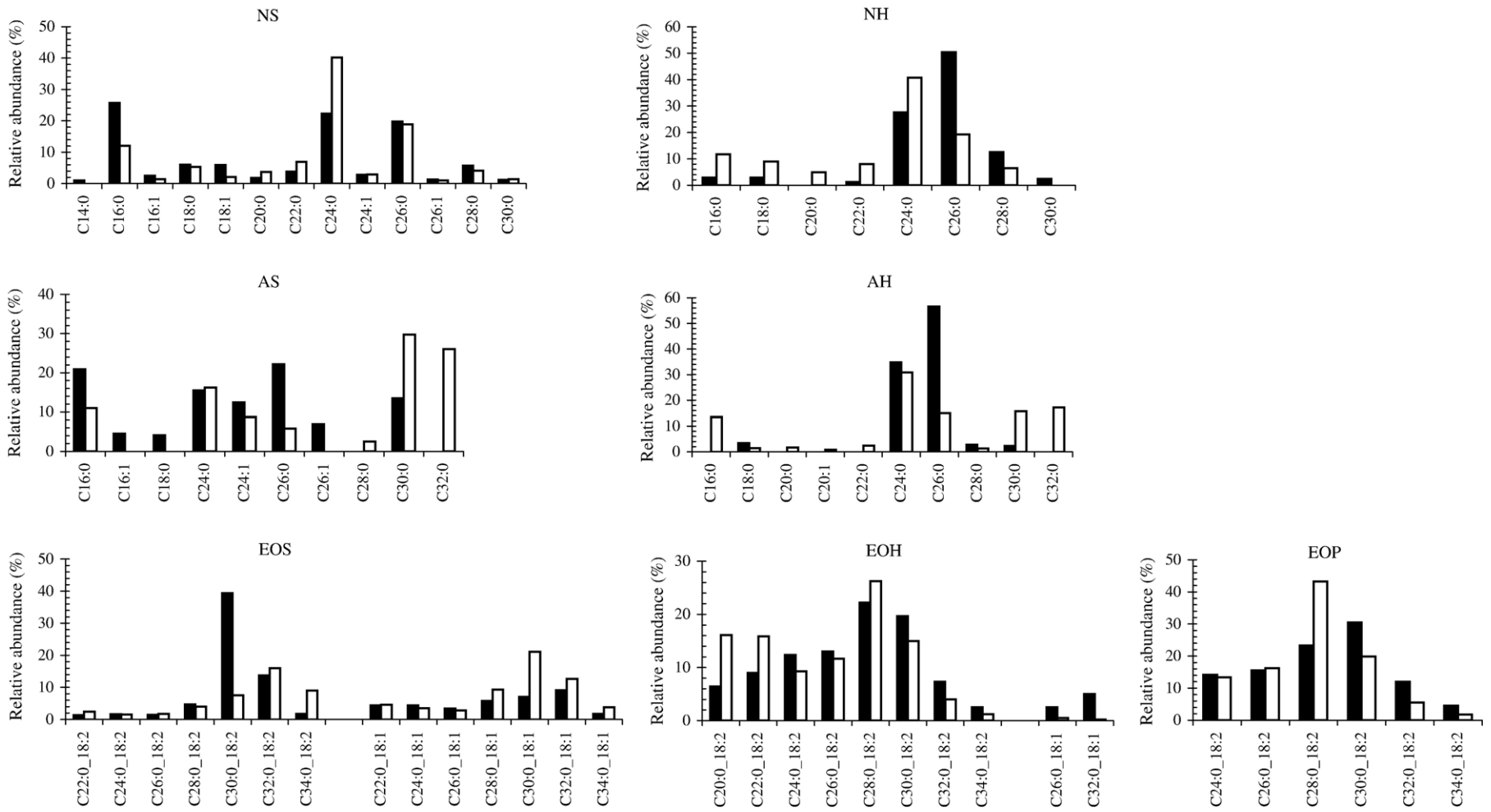

Fig. 4. Molecular species composition of ceramide subclasses. Total lipid extract analysis of ROC (white bars) and human skin (black bars) by mass-spectrometry. Relative abundance: Percent of acyl chain lengths in the respective ceramide class.

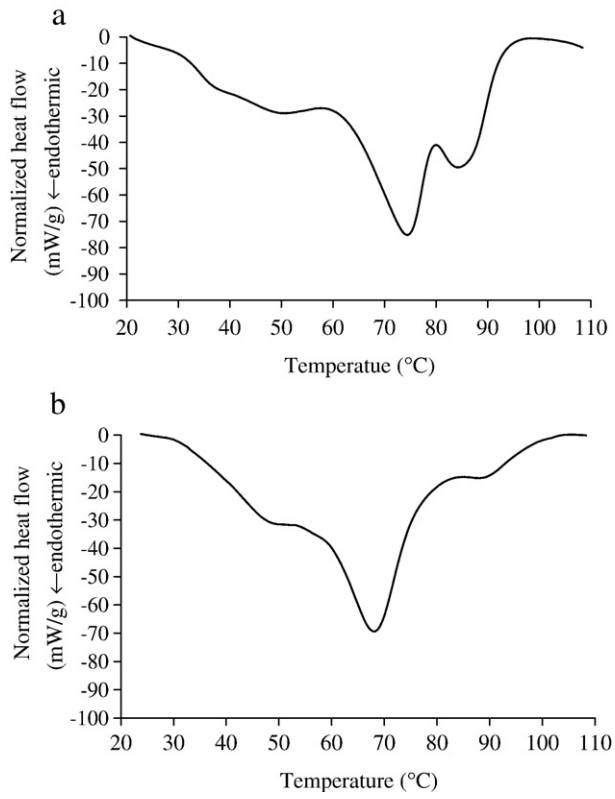

Fig. 5. Representative DSC heating curves of human (a) and ROC (b) stratum corneum. The average transition temperatures and standard deviations are 33.4±1.7; 49.5±2.1; 73.6±1.3; 86.1±1.5 °C for human and 47.2±2.0; 67.5±0.4; 89.0±0.7 °C for ROC stratum corneum, respectively (n=4).

weight, respectively. TLC analysis showed that the stratum corneum from human skin and ROC samples displayed very similar lipid compositions (Fig. 1). The proportions of the three main lipid classes, i.e., ceramides, cholesterol and fatty acids were very similar, albeit the proportion of free fatty acid was slightly reduced in ROC stratum corneum (10% less than in human stratum corneum) (Fig. 2). The level of cholesterol sulfate was significantly higher in ROC stratum corneum (40% more than in human stratum corneum) (Fig. 2). Stratum corneum of both human skin and ROC contained only low amounts of phospholipids, 0.4% and 0.2% of total lipids, respectively. However, in human skin half of the phospholipids were phosphatidylethanolamines, and ROC contained mainly phosphatidylcholine and its alkyl derivatives. There were only trace amounts of glucosylceramides in both samples.

3.2. Ceramide subclass compositions

Mass-spectrometric analysis of the ceramide bands separated by TLC revealed differences in the ceramide subclass compositions of ROC and human skin extracts (Table 1). In ROC, the EOP, NP and AP subclasses were not detectable and band 4 consisted mainly of AS and band 5 (a+b) only of AH, while in human skin, band 4 consisted equally of AS and NH and band 5a equally of AP and AH. TLC quantification of the subclasses revealed that although the total amounts of ceramides in native skin and ROC were similar, the proportions of ceramide subclasses differed clearly (Fig. 3). Ceramides EOP, NP and AP were undetectable in ROC, and it contained more ceramide NS than human skin. Also the content of free EOS was higher in ROC, while the content of ceramides covalently bound to proteins (OS, OH, OP) was significantly lower in ROC, only 1/3 of that in human skin.

Mass-spectrometric analyses indicated that the fatty acid profiles of ceramides NS, AS, NH and AH were generally similar in ROC and human skin, although some differences in relative abundances were observed (Fig. 4). NS ceramide of human skin contained equal amounts of acyl chains C16:0, C24:0 and C26:0, while C24:0 dominated in ROC. In ceramide AS from human skin, the acyl chain length varied from 16 to 30 carbons, while AS from ROC contained mainly C30:0 and C32:0 fatty acids. In NH from human skin, C24:0, C26:0 and C28:0 dominated, while in ROC the average acyl chain length was significantly smaller. In ceramide AH of ROC, acyl chains C16:0–C32:0 were observed, while human skin contained mainly C24:0 and C26:0 chains.

Mass-spectrometric analysis of the total lipid extract indicated the presence EOP in ROC, although this subclass was not apparent in the TLC analysis. The major amide-linked fatty acids of EOP and EOH in both ROC and human stratum corneum were C28:0 and C30:0, respectively, and in both cases the ω-ester-linked chain was linoleic acid (C18:2) (Fig. 4). However, in EOH there were also trace amounts of ω-ester-linked oleic acid in human skin (0.7%) and ROC (7.5%). In EOS, the main amide-linked fatty acid was C30:0 and contained both ester-linked linoleic and oleic acids, but the proportion of linoleic acid was lower in ROC (42%) compared to that found in human skin (64%).

3.3. Differential scanning calorimetry

Four phase transitions (average at 33, 50, 74 and 86 °C) were observed in stratum corneum of human skin and three (average at 47, 68 and 89 °C) in ROC when samples of four different donors and culture batches were analyzed (Fig. 5). The first minor transition (T_1) occurred at 33 °C in native skin, but was absent in ROC. The second small transition (T_x) was observed around 50 °C in both membranes. The main lipid-associated phase transition in human skin occurred at 74 °C (T_2), but at 68 °C in ROC. The high temperature transition (T_3) had a much lower enthalpy in ROC and occurred at a higher temperature (89 °C) than in human skin (86 °C). On reheating, the two lipid transitions T_2 and T_3 coalesced into a single endotherm (detectable as the main peak and the shoulder) at approximately 67 and 72 °C in human skin and ROC, respectively. The T_1 and T_x transitions were not reversible under these conditions.

4. Discussion

Although the lipid composition of skin model cultures has been investigated, these studies have mainly focused on the lipids present in the entire epidermis rather than stratum corneum [18,28,51]. However, the lipid composition changes dramatically from stratum granulosum to stratum corneum. In skin

models, the thickness of the viable epidermis is typically only half of that in human skin, while stratum corneum is about twice as thick, in some cases even 10-fold thicker than in human skin [27,28]. These variations complicate comparisons between models as well as with human skin. This problem can be avoided by analyzing isolated stratum corneum as was done here.

ROC stratum corneum contained cholesterol, ceramides and FFA in almost the same proportions as found in the skin (28 vs 27% cholesterol, 52 vs 51% ceramides, 17 vs 21% FFA for the ROC and human stratum corneum, respectively) (Fig. 2). The epidermal phospholipids were efficiently degraded to free fatty acids and thus mature stratum corneum of ROC, like that of human skin, was found to contain only minute quantities of phospholipids. The lipid composition of the stratum corneum of other reconstructed skin models differs more extensively from human skin (Table 2). For example, the human keratinocyte culture LSE has been reported to contain a higher amount of cholesterol (~66%) and much less ceramides (~27%) and FFA (~7%) compared to human stratum corneum [52].

Lipids in human skin form highly ordered lamellar structures, characterized by a long periodicity phase (LPP) of approx. 13 nm (Table 2) [6]. It is known that cholesterol, free fatty acids and ceramides, especially EOS, are essential components of this structure [10,53]. In human skin, the ω-linked acyl chain in hydroxyceramides is typically linoleic acid (C18:2) which must be obtained from the diet. In essential fatty acid deficiency, linoleate is partially replaced by oleate and this results in skin hyperproliferation and an altered barrier function [54,55]. In the present study, the EOS content of ROC was similar, or slightly higher, to that of the native skin (Fig. 3). The linoleic acid was the only ω-linked acyl moiety in EOH and EOP both in ROC and human skin, while in EOS of ROC linoleic acid represented 42% of total ω-linked chains (Fig. 4). It is still somewhat less than the level present in human skin (64%). In the other skin models which have been investigated (EpiDerm penetration model, EpiDerm irritation model, Episkin penetration model, Episkin irritation model, SkinEthic, RE-DED) the proportion of EOS of total ceramides (8–15%) was reported to be similar to that in human skin (~9%), but LPP (~12 nm) has been found in only a few samples (EpiDerm penetration model, RE-DED) [28]. In skin models, the ω-linked linoleic acid is largely replaced by oleic acid [19,29,56]. Calf serum in the culture medium is the only source of essential fatty acids for the cells, but this contains only low amounts of linoleic acid (18:2) and linolenic acid (18:3) [57,58]. Addition of a mixture of fatty acids (palmitic, linoleic and arachidonic acids) to a serum free culture medium has been reported to improve this situation, but nonetheless only 10–20% of ω-linked acyl chains in hydroxyceramides were in the linoleate form (compared to 70–80% in human skin) [29] (Table 2).

The proportion of ceramide NS in ROC was higher than in native stratum corneum and ceramides NP and AP were not detected (Fig. 3). Ponec and coworkers have analyzed the ceramide profile of a reconstructed human keratinocyte culture (RE-DED) [19,31]. They found higher proportion of NS, lower proportions of AS and AP than in human skin, and the absence of AH, when the cultures were grown in medium without serum but with fatty acid supplementation (i.e. palmitate, linoleinate and

Table 2
Stratum corneum structure analysis of human skin and epidermal skin models

Source	Lipid content of model SC in comparison to human SC	Ceramide subclasses	Linoleate content of EOS (%)	Covalently bound ceramides	LPP (nm)	Thermal phase transitions (DSC) (°C)[1]
Human	CERs (18–41%) CHOL (14–33%) FFAs (9–20%) CS (2–6%)[2]	Nine classes[3]	70–80[2] 64[4]	1.4% of the dry mass	6.4 13.4[6]	36–40[7], 33[4] (T_1) 51[8], 50[4] (T_x) 65–75[7], 74[4] (T_2) 78–85[7], 86[4] (T_3)
ROC[4]	Equal amount of CHOL and CERs, slightly less FFAs, more CS	More NS, absence of NP and AP	42	Present, 1/3 of that in human skin	–	47 (T_x), 68 (T_2), 89 (T_3)
EpiDerm[6]	–	More NS, less AS and AP, absence of AH	–	–	12	–
Episkin	–	More NS, less AS and AP, absence of AH[6]	–	–	nd[9]	–
SkinEthic, CSS[10]	–	More NS, less AS and AP, absence of AH	–	–	–	–
RE-DED	Equal amount of CHOL and CERs, much less FFAs[11]	Almost equal to human skin[6]	10–20[3]	Present, equal amount to human skin[12]	12[6]	–
LSE	More CHOL, much less CERs and FFAs, equal amount of CS[13]	More NS, less AS and AP, absence of AH[14]	–	–	–	–
In-house model[15]	More CHOL, much less CERs and FFAs	–	–	Absent	–	–
In-house model[16]	More CHOL, much less CERs and FFAs	Reduced amount of most polar ceramides	–	Absent	–	58 (T_2)

Data shown is summary of literature reports and the present study. LP = lamellar phases, nd = not detected, [1]hydration level about 20%, [2][74–76], [3][29], [4]present study, [5][12], [6][28], [7][68,77–79], [8][79], [9][27], [10][28,31], [11][80], [12][63], [13][52], [14][31], [15][61], [16][62].

arachidonate). Similar ceramide profiles have been observed for commercial skin models (EpiDerm, SkinEthic, Episkin and LSE) and for an in-house model (cultured skin substitute, CSS) [27,28,31] (Table 2). However, the supplementation of RE-DED medium with vitamin C led to a ceramide profile similar to that of native epidermis [29,31,59]. We have routinely included vitamin C in the culture medium, but these deviations in ceramide composition of ROC might be alleviated by inclusion of suitable fatty acids in the medium.

Morphological studies have reported that ROC contains cornified envelopes in the stratum corneum and these are responsible for the characteristic components of the envelope such as keratin filaments, involucrine and filaggrin [26,36]. We found covalently bound ceramides in stratum corneum of ROC, albeit in lesser amounts (1/3) than in human skin (Fig. 3). On the other hand, ROC seem to contain free ω-hydroxyceramides, even in higher amounts than are present in skin. The lack of some proteins or enzymes essential for keratinocyte differentiation, or the lack of essential fatty acids, respectively, might be responsible for the lower amount of covalently bound ceramides in ROC [15,60]. The presence of covalently bound ceramides in reconstructed skin models has not been widely studied (Table 2). While Kennedy et al. [61] and Pouliot et al. [62] did not find any covalently bound ceramides in their reconstructed human epidermis, Ponec et al. [63] did detect these compounds in amounts comparable with those in native skin.

We observed four endothermic transitions related to lipids in human stratum corneum, i.e. at 33, 50, 74 and 86 °C and three phase transitions in ROC, i.e. at 47, 68 and 89 °C (Fig. 5). The average thermal phase transitions of human stratum corneum from four different donors deviated somewhat from data published on samples with a similar level of hydration (about 20%; Table 2), though the reasons for this are not obvious. Since we were only interested in lipid-associated transitions, the scans were not extended to the high temperatures required to detect protein denaturation. The thermal transition at 33 °C (T_1) may have contributions from contaminating sebaceous lipids [64], the solid-to-fluid transition of a subset of SC lipids [61] and the transformation of an orthorhombic lipid packing to a hexagonal arrangement [65], possibly occurring in different lipid domains within the stratum corneum. Another low temperature transition at approximately 55 °C (T_x) has been attributed to lipids covalently bound to the corneocyte envelope proteins and FTIR measurements indicated that this transition is due to the loss of the crystalline, orthorhombic lattice structure of covalently bound lipids [42,66–68]. ROC did not exhibit the T_1 transition, which may imply that these lipid domains are differently distributed during the thermal keratinocyte differentiation. It is not clear why the T_x transition, tentatively attributed to protein-bound ceramides of ROC (47 °C), occurs at a lower temperature than in native skin (50 °C).

The lipid-associated transitions in human skin at 65–75 °C (T_2) are believed to be due to disordering of a lamellar lipid phase, or more precisely, to a transition from a gel phase to a liquid crystalline phase [6,64,65,68,69]. In the ROC, the T_2 transition occurred at a somewhat lower temperature (at 68 °C) compared to human skin (at 74 °C). This phenomenon may be partly due to the observed differences in lipid composition of ROC, such as the absence of ceramides NP and AP, small differences in fatty acid chain lengths of ceramides and the over-expression of the fraction of oleic acid in ω-hydroxyceramides, all of which can influence lamellar and lateral lipid packing and be reflected in different thermal profiles. The composition of ceramides in artificial mixtures of stratum corneum lipids has been reported to influence thermal behavior, e.g. the diversity of chain lengths of ceramides and FFAs in the model mixture seems to mimic the phase behavior of lipids in intact stratum corneum to a much greater extent [70,71]. As compared to human skin, distinctly lower transition temperatures (17 and 20 °C lower) have been found for two other skin models [61,62]. The lipid arrangement of the RE-DED model, which is believed to have a lipid composition and organization very similar to human skin, is transformed from a hexagonal to liquid crystalline phase at a slightly lower temperature (60–75 °C) than in human skin (65–90 °C) as determined by X-ray diffraction [52]. Also the 12 nm lamellar long periodicity phase (LPP) disappeared at a lower temperature (61–67 °C) than the 13.4 nm LPP of human skin (67–75 °C) [31].

The transition at around 80 °C (T_3) has been attributed to the gel to liquid crystalline phase transformation of protein-bound lipids in the cornified envelope [64,68,69]. In ROC, the T_3 transition occurred at a slightly higher temperature (89 °C) than in human skin (86 °C) (Fig. 5). This phenomenon has not been previously reported in the literature, but it might cause some structural differences in lipid–protein complexes. However, in the ROC the enthalpy of this peak was significantly less, indicative of a lower amount of covalently bound lipids than in skin, in agreement with the TLC data.

We are interested in evaluating the ROC as a potential substitute for human skin in percutaneous absorption and skin irritation studies, and therefore comparison is made in the present and previous experiments with human skin instead of rat skin. Thus, the crucial issue is how successful the ROC model is in mimicking the behavior of human skin with respect to permeation and irritation. Human and rat keratinocytes are different and they do not produce similar permeation barriers. ROC is leakier than human skin but it is significantly less permeable than rat skin [37,72]. The thermal lipid phase transitions of ROC were not identical to either human or rat [67]. Ceramides NP and AP are produced in rat keratinocytes but they were absent in the ROC [73]. Therefore, we would probably reach the same conclusion even if we used rat skin as our comparison. The formation of the cultured stratum corneum is largely governed by the keratinocyte expression profile and differentiation process, and not simply by the cell origin.

REK is a continuous cell line and therefore ROC cultures are easy to prepare, always available, and reproducible. The main advantage of ROC is its well developed permeability barrier, which closely resembles human skin [37]. This is important with respect to solute permeation, permeation enhancement effects, and chemical irritation [37–39]. The lipid matrix constitutes the major barrier to the penetration of drugs and chemicals. Therefore, the differences and similarities in lipid composition and in lipid-associated thermal transitions demonstrated in this study may explain the similar, but not identical permeation barrier of ROC in comparison to human skin. Based

on the observations in this and previous studies, the structure of the stratum corneum in ROC seems to be less ordered and the polar permeation pathway is more predominant than is the case in human skin [39].

In conclusion, ceramides, free fatty acids and cholesterol, which are the most important elements for the formation of the highly ordered structure of stratum corneum lipid domains, were all present in ROC in amounts similar to those found in human skin. The most significant differences were the absence of two ceramide classes, partial substitution of linoleate for oleate in ω-hydroxyceramides and the lower level of bound ceramides. These variations could partly explain the different thermal behavior and somewhat higher permeability of ROC vs human skin. In the future, modifications of the culture conditions, e.g. supplementation with essential fatty acids, may bring the lipid composition and structure of ROC more close to those of human skin. This knowledge of the differences and similarities in the lipid matrix of ROC provides additional information to understand the relevance of results in future studies with this model.

Acknowledgements

This work was supported by the Graduate School ESPOM and the European Union GALENOS project. The authors wish to thank Dr. Seppo Auriola for the professional advice concerning lipid analysis and Dr. Ossi Korhonen for the technical assistance with DSC measurements.

References

[1] P.M. Elias, Epidermal lipids, barrier function, and desquamation, J. Invest. Dermatol. 80 (1983) 44s–49s Suppl.
[2] L. Landmann, Epidermal permeability barrier: transformation lamellar granule-disks into intercellular sheets by a membrane-fusion process, a freeze-fracture study, J. Invest. Dermatol. 87 (1986) 202–209.
[3] P.M. Elias, C. Cullander, T. Mauro, U. Rassner, L. Kömüves, B. Brown, G.K. Menon, The secretory granular cell: the outermost granular cell as a specialized secretory cell, J. Invest. Dermatol. Symp. Proc. 3 (1998) 87–100.
[4] P.M. Elias, Stratum corneum defensive functions: an integrated view, J. Invest. Dermatol. 125 (2005) 183–200.
[5] Y-L. Chen, T.S. Wiedmann, Human stratum corneum lipids have a distorted orthorhombic packing at a surface of cohesive failure, J. Invest. Dermatol. 107 (1996) 15–19.
[6] J.A. Bouwstra, G.S. Gooris, J.A. van der Spek, W. Bras, Structural investigations of human stratum corneum by small-angle X-ray scattering, J. Invest. Dermatol. 97 (1991) 1005–1012.
[7] J.A. Bouwstra, G.S. Gooris, F.E.R. Dubbelaar, M. Ponec, Phase behavior of stratum corneum lipid mixtures based on human ceramides: the role of natural and synthetic ceramide 1, J. Invest. Dermatol. 118 (2002) 606–617.
[8] J.A. Bouwstra, P.L. Honeywell-Nguyen, G.S. Gooris, M. Ponec, Structure of the skin barrier and its modulation by vesicular formulations, Prog. Lipid Res. 42 (2003) 1–36.
[9] M. de Jager, G. Gooris, M. Ponec, J. Bouwstra, Acylceramide head group architecture affects lipid organization in synthetic ceramide mixtures, J. Invest. Dermatol. 123 (2004) 911–916.
[10] V. Schreiner, G.S. Gooris, S. Pfeiffer, G. Lanzendörfer, H. Wenck, W. Diembeck, E. Proksch, J. Bouwstra, Barrier characteristics of different human skin types investigated with X-ray diffraction, lipid analysis, and electron microscopy imaging, J. Invest. Dermatol. 114 (2000) 654–660.
[11] D.C. Swartzendruber, P.W. Wertz, K.C. Madison, D.T. Downing, Evidence that the corneocyte has a chemically bound lipid envelope, J. Invest. Dermatol. 88 (1987) 709–713.
[12] P.W. Wertz, K.C. Madison, D.T. Downing, Covalently bound lipids of human stratum corneum, J. Invest. Dermatol. 92 (1989) 109–111.
[13] P.W. Wertz, The nature of epidermal barrier: biochemical aspects, Adv. Drug Deliv. Rev. 18 (1996) 283–294.
[14] M.E. Stewart, D.T. Downing, The ω-hydroxyceramides of pig epidermis are attached to corneocytes solely through ω-hydroxyl groups, J. Lipid Res. 42 (2001) 1105–1110.
[15] S. Meguro, Y. Arai, Y. Masukawa, K. Uie, I. Tokimitsu, Relationship between covalently bound ceramides and transepidermal water loss (TEWL), Arch. Dermatol. Res. 292 (2000) 463–468.
[16] J. Medina, A. de Brugerolle de Frassinette, S-D. Chibout, M. Kolopp, R. Kammermann, P. Burtin, M-E. Ebelin, A. Cordier, Use of human skin equivalent Apligraf for in vitro assessment of cumulative skin irritation potential of topical products, Toxicol. Appl. Pharmacol. 164 (2000) 38–45.
[17] M. Michel, L. Germain, P.M. Bélanger, F.A. Auger, Functional evaluation of anchored skin equivalent cultured *in vitro*: percutaneous absorption studies and lipid analysis, Pharm. Res. 12 (1995) 455–458.
[18] C. Asbill, N. Kim, A. El-Kattan, K. Creek, P. Wertz, B. Michniak, Evaluation of a human bio-engineered skin equivalent for drug permeation studies, Pharm. Res. 17 (2000) 1092–1097.
[19] M. Ponec, A. Weerheim, J. Kempenaar, A.M. Mommaas, D.H. Nugteren, Lipid composition of cultured human keratinocytes in relation to their differentiation, J. Lipid Res. 29 (1988) 949–961.
[20] C.L. Cannon, P.J. Neal, J.A. Southee, J. Kubilus, M. Klausner, New epidermal model for dermal irritancy testing, Toxicol. In Vitro 8 (1994) 889–891.
[21] M. Rosdy, L.C. Clauss, Terminal epidermal differentiation of human keratinocytes grown in chemically defined medium on inert filter substrates at the air–liquid interface, J. Invest. Dermatol. 95 (1990) 409–414.
[22] R. Roguet, C. Cohen, K.G. Dossou, A. Rougier, Episkin, a reconstructed human epidermis for assessing in vitro the irritancy of topically applied compounds, Toxicol. In Vitro 8 (1994) 283–291.
[23] E. Bell, N. Parenteau, R. Gay, C. Nolte, P. Kemp, P. Bilbo, B. Ekstein, E. Johnson, The living skin equivalent: its manufacture, its organotypic properties and its responses to irritants, Toxicol. In Vitro 5 (1991) 591–596.
[24] V.H.W. Mak, M.B. Cumpstone, A.H. Kennedy, C.S. Harmon, R.H. Guy, R.O. Potts, Barrier function of human keratinocyte cultures grown at air–liquid interface, J. Invest. Dermatol. 96 (1991) 323–327.
[25] Y. Poymay, F. Dupont, S. Marcoux, M. Leclercq-Smekens, M. Hérin, A. Coquette, A simple reconstructed human epidermis: preparation of the culture model and utilization in in vitro studies, Arch. Dermatol. Res. 296 (2004) 203–211.
[26] S. Pasonen-Seppänen, T.M. Suhonen, M. Kirjavainen, E. Suihko, A. Urtti, M. Miettinen, M. Hyttinen, M. Tammi, R. Tammi, Vitamin C enhances differentiation of a continuous keratinocyte cell line (REK) into epidermis with normal stratum corneum ultrastructure and functional permeability barrier, Histochem. Cell Biol. 116 (2001) 287–297.
[27] M. Ponec, E. Boelsma, A. Weerheim, A. Mulder, J. Bouwstra, M. Mommaas, Lipid and ultrastructural characterization of reconstructed skin models, Int. J. Pharm. 203 (2000) 211–225.
[28] M. Ponec, E. Boelsma, S. Gibbs, M. Mommaas, Characterization of reconstructed skin models, Skin Pharmacol. Appl. Skin Physiol. 15 (2002) 4–17.
[29] M. Ponec, A. Weerheim, P. Lankhorst, P. Wertz, New acylceramide in native and reconstructed epidermis, J. Invest. Dermatol. 120 (2003) 581–588.
[30] S. Gibbs, J. Vicanová, J. Bouwstra, D. Valstar, J. Kempenaar, M. Ponec, Culture of reconstructed epidermis in a defined medium at 33 °C shows a delayed epidermal maturation, prolonged lifespan and improved stratum corneum, Arch. Dermatol. Res. 289 (1997) 585–595.
[31] M. Ponec, A. Weerheim, J. Kempenaar, A. Mulder, G.S. Gooris, J. Bouwstra, A.M. Mommaas, The formation of competent barrier lipids in reconstructed human epidermis requires the presence of vitamin C, J. Invest. Dermatol. 109 (1997) 348–355.

[32] H. Wagner, K-H. Kostka, C-M. Lehr, U.F. Schaefer, Interrelation of permeation parameters obtained from in vitro experiments with human skin and skin equivalents, J. Control. Release 75 (2001) 283–295.
[33] F.P. Schmook, J.G. Meingassner, A. Billich, Comparison of human skin or epidermis models with human and animal skin in-vitro percutaneous absorption, Int. J. Pharm. 215 (2001) 51–56.
[34] F. Dreher, F. Fouchard, C. Patouillet, M. Andrian, J-T. Simonnet, F. Benech-Kieffer, Comparison of cutaneous bioavailability of cosmetic preparations containing caffeine or α-tocopherol applied on human skin models or human skin ex vivo at finite doses, Skin Pharmacol. Appl. Skin Physiol. 15 (2002) 40–58.
[35] C. Lotte, C. Ptouillet, M. Zanina, A. Messager, R. Roguet, Permeation and skin absorption: reproducibility of various industrial reconstructed human skin models, Skin Pharmacol. Appl. Skin Physiol. 15 (2002) 18–30.
[36] S. Pasonen-Seppänen, T.M. Suhonen, M. Kirjavainen, M. Miettinen, A. Urtti, M. Tammi, R. Tammi, Formation of permeability barrier in epidermal organotypic culture for studies on drug transport, J. Invest. Dermatol. 117 (2001) 1322–1324.
[37] T.M. Suhonen, S. Pasonen-Seppänen, M. Kirjavainen, M. Tammi, R. Tammi, A. Urtti, Epidermal cell culture model derived from rat keratinocytes with permeability characteristics comparable to human cadaver skin, Eur. J. Pharm. Sci. 20 (2003) 107–113.
[38] S. Pappinen, S. Pasonen-Seppänen, M. Suhonen, R. Tammi, A. Urtti, Rat epidermal keratinocyte organotypic culture (ROC) as a model for chemically induced skin irritation testing, Toxicol. Appl. Pharmacol. 208 (2005) 233–241.
[39] S. Pappinen, S. Tikkinen, S. Pasonen-Seppänen, L. Murtomäki, M. Suhonen, A. Urtti, Rat epidermal keratinocyte organotypic culture (ROC) compared to human cadaver skin: the effect of skin permeation enhancers, Eur. J. Pharm. Sci. 30 (2007) 240–250.
[40] L. Paasonen, M. Korhonen, M. Yliperttula, A. Urtti, Epidermal cell culture model with tight stratum corneum as a tool for dermal gene delivery studies, Int. J. Pharm. 307 (2006) 188–193.
[41] H.P. Baden, J. Kubilus, The growth and differentiation of cultured newborn rat keratinocytes, J. Invest. Dermatol. 80 (1983) 124–130.
[42] C.L. Gay, R.H. Gay, G.M. Golden, V.H.W. Mak, M.L. Francoeur, Characterization of low-temperature (i.e., <65 °C) lipid transitions in human stratum corneum, J. Invest. Dermatol. 103 (1994) 233–239.
[43] S. Law, P.W. Wertz, D.C. Swartzendruber, C.A. Squier, Regional variation in content, composition and organization of porcine epithelial barrier lipids revealed by thin-layer chromatography and transmission electron microscopy, Arch. Oral Biol. 40 (1995) 1085–1091.
[44] J. Folch, M. Lees, G.G.S. Stanley, A simple method for the isolation and purification of total lipids from animal tissues, J. Neurochem. 4 (1959) 9–18.
[45] P.W. Wertz, D.T. Downing, Metabolism of linoleic acid in porcine epidermis, J. Lipid Res. 31 (1990) 1839–1844.
[46] A.H. Merrill Jr., M.C. Sullards, J.C. Allegood, S. Kelly, E. Wang, Sphingolipidomics: high-throughput, structure-specific, and quantitative analysis of sphingolipids by liquid chromatography tandem mass spectrometry, Methods 36 (2005) 207–224.
[47] P. Haimi, A. Uphoff, M. Hermansson, P. Somerharju, Software tools for analysis of mass spectrometric lipidome data, Anal. Chem. 78 (2006) 8324–8331.
[48] M. Koivusalo, P. Haimi, L. Heikinheimo, R. Kostiainen, P. Somerharju, Quantitative determination of phospholipid compositions by ESI-MS: effects of acyl chain length, unsaturation, and lipid concentration on instrument response, J. Lipid Res. 42 (2001) 663–672.
[49] J. Bouwstra, G.S. Gooris, W. Bras, D.T. Downing, Lipid organization in pig stratum corneum, J. Lipid Res. 36 (1995) 685–695.
[50] G.M. Golden, D.B. Guzek, A.H. Kennedy, J.E. McKie, R.O. Potts, Stratum corneum lipid phase transitions and water barrier properties, Biochemistry 29 (1987) 2382–2388.
[51] M. Fartasch, M. Ponec, Improved barrier structure formation in air-exposed human keratinocyte culture systems, J. Invest. Dermatol. 102 (1994) 366–374.
[52] J.A. Bouwstra, G.S. Gooris, A. Weerheim, J. Kempenaar, M. Ponec, Characterization of stratum corneum structure in reconstructed epidermis by X-ray diffraction, J. Lipid Res. 36 (1995) 496–504.
[53] J.A. Bouwstra, G.S. Gooris, F.E.R. Dubbelaar, M. Ponec, Phase behaviour of lipid mixtures based on human ceramides: coexistence of crystalline and liquid phases, J. Lipid Res. 42 (2001) 1759–1770.
[54] P.W. Wertz, E.S. Cho, D.T. Downing, Effect of essential fatty acid deficiency on the epidermal sphingolipids of the rat, Biochim. Biophys. Acta 753 (1983) 350–355.
[55] H.S. Hansen, B. Jensen, Essential function of linoleic acid esterified in acylglucosylceramide and acylceramide in maintaining the epidermal water permeability barrier. Evidence from feeding studies with oleate, linoleate, arachidonate, columbinate and α-linolenate, Biochim. Biophys. Acta 834 (1985) 357–363.
[56] J. Vicanová, A.M. Weerheim, J.A. Kempenaar, M. Ponec, Incorporation of linoleic acid by cultured human keratinocytes, Arch. Dermatol. Res. 291 (1999) 405–412.
[57] R.R. Isseforoff, V.A. Zoboh, R.S. Chapkin, D.T. Martinez, Conversion of linoleic acid into arachidonic acid by cultured murine and human keratinocytes, J. Lipid Res. 28 (1987) 1342–1349.
[58] A.A. Spector, S.N. Mathur, T.L. Kaduce, B.T. Hyman, Lipid nutrition and metabolism of cultured mammalian cells, Prog. Lipid Res. 19 (1981) 155–186.
[59] I.L.A. Boxman, J. Kempenaar, E. de Haas, M. Ponec, Introduction of HSP27 nuclear immunoreactivity during stress is modulated by vitamin C, Exp. Dermatol. 11 (2002) 509–517.
[60] E. Candi, R. Schmidt, G. Melino, The cornified envelope: a model of cell death in the skin, Nat. Rev. Mol. Cell Biol. 6 (2005) 328–340.
[61] A.H. Kennedy, G.M. Golden, C.L. Gay, R.H. Gay, M.L. Francoeur, V.H. W. Mak, Stratum corneum lipids of human epidermal keratinocyte air–liquid cultures: implications for barrier function, Pharm. Res. 13 (1996) 1162–1167.
[62] R. Pouliot, L. Germain, F.A. Auger, N. Tremblay, J. Juhasz, Physical characterization of the stratum corneum on an in vitro human skin equivalent produced by tissue engineering and its comparison with normal human skin by ATR-FTIR spectroscopy and thermal analysis (DSC), Biochim. Biophys. Acta 1439 (1999) 341–352.
[63] M. Ponec, E. Boelsma, A. Weerheim, Covalently bound lipids in reconstructed human epithelia, Acta Derm. Veneorol. 80 (2000) 89–93.
[64] G.M. Golden, D.B. Guzek, R.R. Harris, J.E. McKie, R.O. Potts, Lipid thermotropic transitions in human stratum corneum, J. Invest. Dermatol. 86 (1986) 255–259.
[65] J.A. Bouwstra, G.S. Gooris, M.A. Salomons-de Vries, J.A. van der Spek, W. Bras, Structure of human stratum corneum as a function of temperature and hydration: a wide-angle X-ray diffraction study, Int. J. Pharm. 84 (1992) 205–216.
[66] C.L. Silva, S.C.C. Nunes, M.E.S. Eusébio, J.J.S. Sousa, A.A.C.C. Pais, Study of human stratum corneum and extracted lipids by thermomicroscopy and DSC, Chem. Phys. Lipids 140 (2006) 36–47.
[67] S.M. Al-Saidan, B.W. Barry, A.C. Williams, Differential scanning calorimetry of human and animal stratum corneum membranes, Int. J. Pharm. 168 (1998) 17–22.
[68] P.A. Cornwell, B.W. Barry, J.A. Bouwstra, G.S. Gooris, Modes of action of terpene penetration enhancers in human skin; differential scanning calorimetry, small-angle X-ray diffraction and enhancer uptake studies, Int. J. Pharm. 127 (1996) 9–26.
[69] S.J. Rehfeld, W.Z. Plachy, S.E. Hou, P.M. Elias, Localization of lipid microdomains and thermal phenomena in murine stratum corneum and isolated membranes complexes: an electron spin resonance study, J. Invest. Dermatol. 95 (1990) 217–223.
[70] B. Glombitza, C.C. Müller-Goymann, Influence of different ceramides on the structure of in vitro model lipid systems of the stratum corneum lipid matrix, Chem. Phys. Lipids 117 (2002) 29–44.
[71] J. Bouwstra, G.S. Gooris, K. Cheng, A. Weerheim, W. Bras, M. Ponec, Phase behavior of isolated skin lipids, J. Lipid Res. 37 (1996) 999–1011.
[72] B. van Ravenzwaay, E. Leibold, The significance of in vitro rat skin absorption studies to human risk assessment, Toxicol. In Vitro 18 (2004) 219–225.
[73] P.W. Wertz, D.T. Downing, R.K. Freinkel, T.N. Traczyk, Sphingolipids of the stratum corneum and lamellar granules of fetal rat epidermis, J. Invest. Dermatol. 83 (1984) 193–195.

[74] M.A. Lampe, M.L. Williams, P.M. Elias, Human epidermal lipids: characterization and modulations during differentiation, J. Lipid. Res. 24 (1983) 131–140.
[75] P.W. Wertz, D.C. Swartzendruber, K.C. Madison, D.T. Downing, Composition and morphology of epidermal cyst lipids, J. Invest. Dermatol. 89 (1987) 419–425.
[76] P.W. Wertz, D.T. Downing, Stratum corneum: biological and biochemical considerations, In: J. Hadgraft, R.H. Gay (Eds.), Transdermal drug delivery: developmental issues and research initiatives, Marcel Dekker, Inc., New York, 1989, pp. 1–22.
[77] B.F. Van Duzee, Thermal analysis of human stratum corneum, J. Invest. Dermatol. 65 (1975) 404–408.
[78] H. Tanojo, J.A. Bouwstra, H.E. Junginger, H.E. Bodde, In vitro human skin barrier modulation by fatty acids: skin permeation and thermal analysis studies, Pharm. Res. 14 (1997) 42–49.
[79] H.K. Vaddi, P.C. Ho, Y.W. Chan, S.Y. Chan, Terpenes in ethanol: haloperidol permeation and partition through human skin and stratum corneum changes, J. Control. Release 81 (2002) 121–133.
[80] M. Ponec, Skin constructs for replacement of skin tissue for in vitro testing, Adv. Drug Deliv. Rev. 54 (2002) S19–S30.